

Original Research

The Catalysts of Au(x)/CuCeO₂ for Preferential Oxidation of Carbon Monoxide and Dynamics in Hydrogen Rich Atmosphere Potentially Applied in Fuel Cell

Yuanyang Zhang*, Yucui Hao, Licong Meng

School of New Materials and Chemical Engineering, Tangshan University, Tangshan 063000, China

Received: 17 January 2022

Accepted: 9 March 2022

Abstract

A series of CuO-CeO₂ catalysts were prepared by coprecipitation method which were characterized by BET, XRD and TPR, respectively. The activity of the prepared catalysts for preferential oxidation of CO was evaluated in a fixed bed reactor. TPR showed that the catalysts of CuO-CeO₂ mainly appeared two characteristic peaks at the range of 60~400°C, i.e. low temperature α peak (160~180°C) and high temperature β peak (180~200°C). The ratio of $\alpha/(\alpha+\beta)$ was the largest when the content of Cu was 8.4(wt.%) on CuO-CeO₂ samples, i.e. the catalyst of Cu(8.0)CeO, which was consistent with that its best activity under used experimental conditions. A series of catalysts of Au(x)/Cu(8.0)CeO were prepared by using Cu(8.0)CeO as precursor with impregnation method. SEM characterization showed that Au could evenly distributed on Cu(8.0)CeO with nano size under the prepared experimental conditions. The activity over the prepared series of Au(x)/Cu(8.0)CeO catalysts for selective oxidation removal of CO showed that it was increased with increasing Au loading, while its activity of Au(x)/Cu(8.0)CeO catalysts did not increase significantly when the Au loading was increased from 0.52(wt.%) to 0.78(wt.%) , which indicated that the appropriate content of Au was 0.52(wt.%) on Cu(8.0)CeO, i.e. Au(0.5)/Cu(8.0)CeO. The oxidation dynamics of CO and H₂ over Au(0.5)/Cu(8.0)CeO was measured in a gradientless reactor and the multiple kinetic regression equations of the oxidation reactions of CO and H₂ were obtained, respectively, which provided the basis for the further study of preferential oxidation of CO performed on Au(0.5)/Cu(8.0)CeO.

Keywords: dynamics, hydrogen energy, CO preferential oxidation, fuel cell

*e-mail: yyzhang90@126.com

Introduction

A considerable effort has been expended in developing technologies for using renewable energy sources. Hydrogen is considered one of the most important environmentally friendly energy carriers [1, 2]. The amount of energy produced per unit mass during hydrogen combustion is higher than that evolved by other fuel such as methane, biomass, gasoline or coal [3-8]. Among the various processes proposed for hydrogen production, the partial oxidation and the steam reforming processes have been attractively used to generate hydrogen from hydrocarbon fuels, such as gasoline, natural gas, or methanol [9-12]. Due to the increasing concerns regarding proton exchange membrane (PEM) fuel cell technology, the selective removal of carbon monoxide in hydrogen-rich gas has attracted much attention recently. Since carbon monoxide is always present in the gas mixture produced from these hydrocarbon fuels, it must be reduced to a level less than 10 ppm in order to avoid rapid deactivation of the platinum electro-catalyst in the fuel cells [13, 14]. The so obtained H₂-rich stream contains 0.5–1.0 vol.% CO, which is a poison for the fuel cell anode catalyst (Pt) [15-17]. The carbon monoxide level of the gases can be reduced by the shift reaction, but such reaction is generally incapable of reducing the carbon monoxide content of the gases much below about 0.2%. Therefore, the preferential oxidation (PROX) of carbon monoxide may be the most suitable method to reduce the amount of carbon monoxide to a suitable level for use in electrochemical fuel cells [18-22]. CO-PROX catalysts have been studied to work under steady-state conditions and have been designed and selected to ensure high CO oxidation activity, selectivity, and stability. Researchers attempted to find a new catalyst with high activity for carbon monoxide removal and with small hydrogen consumption. Pt/Al₂O₃ was firstly proposed as an effective catalyst for selective oxidation of carbon monoxide in the presence of excess hydrogen. Platinum supported on zeolite catalysts could oxidize carbon monoxide much more selectively in a large excess of hydrogen with the addition of a low concentration of oxygen than a conventional Pt/Al₂O₃ catalyst [23]. Several works showed that Ru/Al₂O₃ was a more efficient catalyst than a currently used Pt/Al₂O₃ [24-26]. Au/Fe₂O₃ offered superior activity and selectivity to Pt/Al₂O₃ at low temperature and high carbon monoxide concentration because steady-state coverage of carbon monoxide on the gold surface was below saturation [27, 28]. Although such advances have been made to enhance the catalytic performance, their performances are not good enough to reduce the carbon monoxide content to below 10 ppm, therefore, multi-stage PROX is still a necessity. Copper/ceria catalysts have been proposed as an alternative due to their good activity and selectivity at low temperatures. It has been suggested that well dispersed CuO over reducible CeO₂ at comparatively low temperature in relation to

bulk CuO is the reason for better CO-PROX activity. This catalyst exhibits high activity and oxidation selectivity at reasonably low temperatures. Additionally, it has been shown that the redox processes regarding CO oxidation involves the reduction and oxidation of both the Cu and CeO₂ species [29-33].

Currently, the narrow temperature range of total CO conversion, unsatisfactory low-temperature activity and poor selectivity at the temperature above 110°C still prevent CuO-CeO₂ based catalysts from practical applications. Centering on the problems of CuO-CeO₂ based catalysts, a great deal of work, including improvement of preparation technology, composition optimization, additive modification and carrier promotion, has been performed recently. Especially, it has been found that the addition of proper promoters can significantly improve catalytic properties of CuO-CeO₂ based catalysts for CO selective oxidation. As a promoter, the addition of Zr into CuO-CeO₂ catalysts resulted in stronger synergistic interaction between copper and ceria, easier reducibility of active copper species and increase of oxygen vacancies and active sites, which has a beneficial effect on the catalytic performance. As reported, Cu-Zr-Ce mixed oxides for selective oxidation of CO had relatively high selectivity and wide temperature span of 40°C for CO complete conversion with the addition of Zr. Meanwhile, the performance of Zr-doped CuO-CeO₂ catalysts could be further improved through the change of preparation technology [34-36].

This paper firstly explored and synthesized series of CuO-CeO₂ nano catalysts and then Au was used to modify its surface on the purpose of coupling the performance of Au and CuO-CeO₂ as well as decreasing the content of the active component of noble metal Au as much as possible, while it could effectively removal of CO in hydrogen rich system under mild conditions through selective catalytic oxidation method. Furthermore, the reaction kinetics of Au (x)/CuCeO₂ catalyst with good performance of selective catalytic removal of CO from hydrogen rich system was measured in a gradientless reactor without internal and external diffusion effects, which would provide the basis for further reactor simulation, process optimization and catalyst engineering design.

Material and Methods

Catalyst Preparation

The catalysts of CuO-CeO₂ were prepared by coprecipitation method. A certain amount of cerium (III) nitrate hexahydrate (AR, ≥99.0%, Sinopharm) and copper (II) nitrate trihydrate (AR, ≥99.0%, Sinopharm) were dissolved to an appropriate amount of deionized water, respectively, which was stirred continuously in a constant temperature water bath at 45°C until dissolved completely. After that, it was still

stirred for 10~30 min. The aqueous solution containing cerium (III) nitrate hexahydrate was firstly transferred into a four mouth flask, and the prepared alkali solution containing sodium hydroxide (AR, ≥98.0%, Sinopharm) and sodium hydrogen carbonate (AR, ≥99.5%, Sinopharm) as well as the copper (II) nitrate trihydrate solution were transferred into the constant pressure funnel, respectively. After that, the solution of alkali solution and copper (II) nitrate trihydrate was added dropwise to four mouth flask under continuously mechanical stirring, respectively, which was kept at constant temperature oil bath at 75°C. The pH value of the solution in the four port flask was controlled at the range of 9~10. After the dropping was finished, the mixture in the four port flask was transferred to a reactor with PTFE coating and crystallized at 95°C for 10 hours. Then, filtered, washed, dried and calcined 2 h at 350°C through program temperature with a heating rate of 2°C/min. The different compositions of CuO-CeO₂ catalysts could be prepared by similar method. Furthermore, the solution with different concentration of hydrogen tetrachloroaurate (III) trihydrate (AR, ≥99.99%, Sinopharm) was prepared, respectively, and the catalysts of Au/CuCeO₂ were prepared by impregnation method by using CuO-CeO₂ as the precursor, which was continuously stirred at a constant temperature water bath at 45°C for 4 h. Then, the excess aqueous solution of sodium borohydride (AR, ≥98.0%, Sinopharm) with a concentration of 40 mm was added for reduction lasted for 4h. The solid was filtered, washed and dried, respectively. The catalysts of Au (x)/CuCeO₂ with different content of Au on CuO-CeO₂ precursor could be prepared by using similar method.

Characterization

Scanning electron microscope (SEM) was conducted on JSM-6330F (Japan) field emission SEM with working voltage of 200kV and resolution of 1.5 nm. X-ray diffractometer (XRD) was determined by D/max 2550 (Japan). CuKα X-ray, 40kV of tube voltage and 100mA of tube current, respectively, with 0.02°·min⁻¹ scanning step at the range of 10~100°. The active components were analyzed by IRIS (HR) plasma atomic emission spectrometer (ICP, USA). The specific surface area and pore structure was measured by ASAP 2020 specific surface and pore structure analyzer (USA). The temperature programmed reduction (TPR) was conducted on temperature programmed reduction instrument (Chembet Pulsar, USA) and the reaction gas was detected by GAM 200 gas mass spectrometer (Inprocess Instruments, Germany).

Evaluation of Catalyst Performance

The oxidative removal of CO was studied in a fixed bed reactor at atmospheric pressure. The inner diameter of the reactor was 8.0mm. The shaped prepared catalyst

with size of 0.20~0.40mm was loaded at the constant temperature zone of the reactor and the lower and upper parts of the catalyst were filled with inactive quartz sand calcined at high temperature, respectively. The system was pre-purged with high purity nitrogen lasted for 1~2 h at 150°C and space velocity of 2500 h⁻¹, respectively, before the removal of CO oxidation experiment and then the reactor temperature was adjusted to the testing reaction temperature. For simplicity, high-purity gases of H₂, O₂, CO and CO₂ (99.999%) were used as reactants, and the flow rate of each gas was controlled by flowmeter, respectively. The mixture of reactant gases through the mixer and preheater, respectively, could either enter the reactor or switch to the chromatograph for analysis of its compositions. The basic experimental conditions were as follows, 80~120°C of the reaction temperature, probably loadings of 0.5 g catalyst, and 5000 h⁻¹ of the gas space velocity, respectively. The basic compositions of reaction gases were controlled by simulating steam reforming and partial oxidation of hydrocarbons for hydrogen production, i.e. H₂: ~75%, CO₂: ~25%, CO: ~ 0.4%, O₂: ~0.6%, respectively. The reaction kinetics of Au (x)/CuCeO₂ catalyst with good performance of selective catalytic removal of CO from hydrogen rich system was measured on Berty Reactor (Autoclave Engineers, USA) without internal and external diffusion effects.

Analytical Methods

Two on-line chromatographs (GC4000, Beijing Dongxi Analytical Instrument Co., Ltd, China) with thermal conductivity detector (TCD) to quantitatively analyze H₂, O₂, Co, CO₂ and low-carbon hydrocarbons such as CH₄, respectively. One chromatographic column was installed with polar packing (Hayesep Q) to analyze CO₂ at 80°C of the column temperature. The other chromatographic column was installed with molecular sieve (5A molecular sieve) to analyze H₂, O₂, CO and CH₄, respectively, at 60°C of the column temperature.

Results and Discussion

Catalytic Removal of CO on CuO-CeO₂

ICP analysis and BET characterization of a series of prepared CuO-CeO₂ catalysts was shown in Table 1. BET results indicated that the specific surface area and pore volume initially increased slightly with the increasing Cu content. While the specific surface area and pore volume of the sample was reached to maximum when the content of Cu was 8.4% under the used preparation conditions. It further indicated that the specific surface area and pore volume of CuO-CeO₂ samples decreased slightly when the content of Cu reached to 12.3%. However, the varied range

Table 1. ICP analysis and BET characterization on CuO-CeO₂ samples.

Samples	Cu content (wt.%)	BET characterization	
		Specific surface area (m ² /g)	Pore volume (cm ³ /g)
Cu(2.0)CeO	2.3	201	0.248
Cu(4.0)CeO	4.5	211	0.274
Cu(8.0)CeO	8.4	224	0.326
Cu(12.0)CeO	12.3	219	0.311

of the specific surface area and pore volume was not changed very much generally.

XRD characterization on the prepared typical catalysts of CuO-CeO₂ was conducted. For simplicity, Fig. 1 only showed the XRD characterization of the two representative catalyst samples with Cu content of 2.3% and 12.3%, respectively. XRD characterization indicated that the crystal structure of the series of CuO-CeO₂ samples did not change with the increasing content of Cu except that the characteristic peak value of XRD was changed under prepared conditions, which provided the basis for comparing their performance on catalytic removal of CO under the almost same conditions.

The effect of Cu content on the performance of CuCeO catalysts over CO catalytic oxidation was shown in Fig. 2, which indicated that the catalysts of CuCeO had relatively good activity on catalytic oxidation removal of CO under experimental conditions.

Furthermore, it indicated that the activity of the catalysts increased with Cu content at the beginning and then decreased slightly with further increasing content of Cu. It showed that the catalyst of Cu(8.0)CeO with 8.4 (wt.%) content of Cu (Table 1) had the best catalytic activity on removal of CO under used experimental conditions. The reason of appearing this phenomenon could be that when the Cu content was further

increased in the sample, it could lead to agglomeration of the active component of CuOx, thus resulting in the reduction of the active number of catalytic reaction and the catalytic activity of CuCeO catalysts would be decreased with further increasing content of Cu in the samples of CuCeO [34-36].

The temperature programmed reduction (TPR) over the series of CuO-CeO₂ catalysts was conducted at the temperature range of 60~400°C. The characterization indicated that the curve mainly appeared two characteristic peaks, which were defined as low temperature α peak (160~180°C) and high temperature β peak (180~200°C), respectively. Probably, the peaks of α and β were corresponding to the reduction of CuOx nano clusters highly dispersed on the surface and the crystal lattice structure of Cu-[Ox]-Ce, respectively. Furthermore, the highly dispersed CuOx nano clusters on the surface would be mainly contributed to the catalytic oxidation of CO [30, 37]. The area of the peaks over α and β appearing on TPR curve was integrated and the ratio of $\alpha/(\alpha+\beta)$ was also calculated and results were shown in Table 2, which indicated that the peak area ratio of $\alpha/(\alpha+\beta)$ was 0.263, 0.322, 0.353 and 0.337 corresponding to the samples of Cu(2.0)CeO, Cu(4.0)CeO, Cu(8.0)CeO and Cu(12.0)CeO, respectively. The experimental results also showed that the activity of Cu(8.0)CeO catalyst had the best performance over

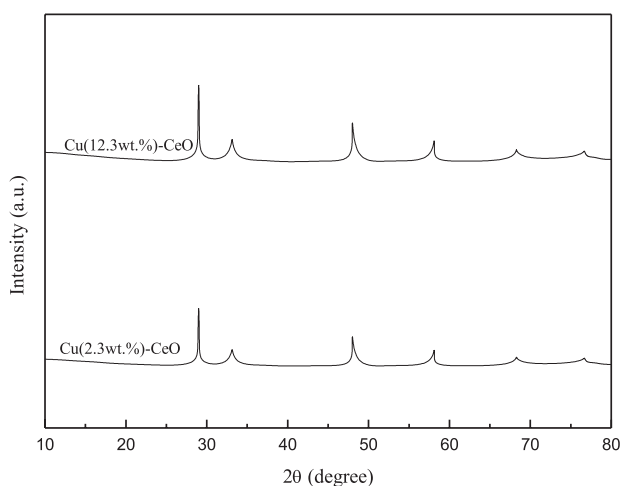
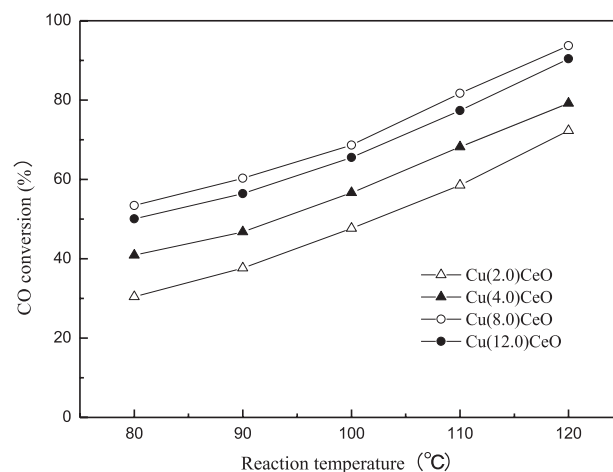
Fig. 1. XRD characterization on the typical prepared CuO-CeO₂ samples.Fig. 2. The comparison on catalytic removal CO performed over CuO-CeO₂ samples.

Table 2. H₂-TPR peak position, area and the ratio of area over CuO-CeO₂ samples.

Samples	Peak position (°C)		Relative peak area		Ratio of peak area
	α	β	α	β	$\alpha/(\alpha+\beta)$
Cu(2.0)CeO	168	182	440	1230	0.263
Cu(4.0)CeO	172	184	670	1410	0.322
Cu(8.0)CeO	174	185	856	1568	0.353
Cu(12.0)CeO	178	192	1060	2080	0.337

Table 3. ICP analysis and BET characterization over Au (x)/Cu (8.0)CeO samples.

Samples	Au content (wt.%)	BET characterization	
		Specific surface area (m ² /g)	Pore volume (cm ³ /g)
Au(0.1)/Cu(8.0)CeO	0.13	223	0.314
Au(0.3)/Cu(8.0)CeO	0.35	220	0.308
Au(0.5)/Cu(8.0)CeO	0.52	210	0.289
Au(0.8)/Cu(8.0)CeO	0.78	208	0.280

catalytic removal of CO at used experimental conditions (Fig. 2), which was basically consistent with the results reported in the literature [38].

Catalytic Removal of CO on Au(x)/Cu(8.0)CeO

The analysis of ICP and BET over samples of Au(x)/Cu(8.0)CeO was shown in Table 3, which indicated that the specific surface area and pore volume decreased slightly with the increase of Au content on the precursor of Cu(8.0)CeO while the variation was not obvious under the prepared conditions.

The surface morphology of the prepared representative Au(x)/Cu(8.0)CeO samples, the content of Au with 0.13 wt.% and 0.78 wt.%, characterized by SEM was shown in Fig. 3, respectively. SEM results showed that the content of Au in the range of 0.1~0.8 wt.% could be evenly distributed on the surface of Cu(8.0)CeO with nano size.

The performance on catalytic removal of CO over series of catalysts of Au(x)/Cu(8.0)CeO was shown in Fig. 4, respectively. The results indicated that the modification of Cu(8.0)CeO sample with Au obviously improved its activity on catalytic removal of CO compared with results shown in Fig. 2. It also showed that the activity of Au(x)/Cu(8.0)CeO catalysts was increased significantly with the increasing Au loadings under the experimental conditions. It seemed that its activity of Au(x)/Cu(8.0)CeO catalysts did not increase obviously when the loading of Au was increased from 0.52 (wt.%) to 0.78 (wt.%). Furthermore, the experimental results indicated that the concentration of CO at outlet of the reactor was less than 10ppm when the reaction temperature was close to 110°C with using catalysts of Au(0.3)/Cu(8.0)CeO, Au(0.5)/Cu(8.0)CeO and Au(0.8)/Cu(8.0)CeO, respectively, with the typical reaction gases by simulating the basic compositions of hydrogen production system through steam reforming

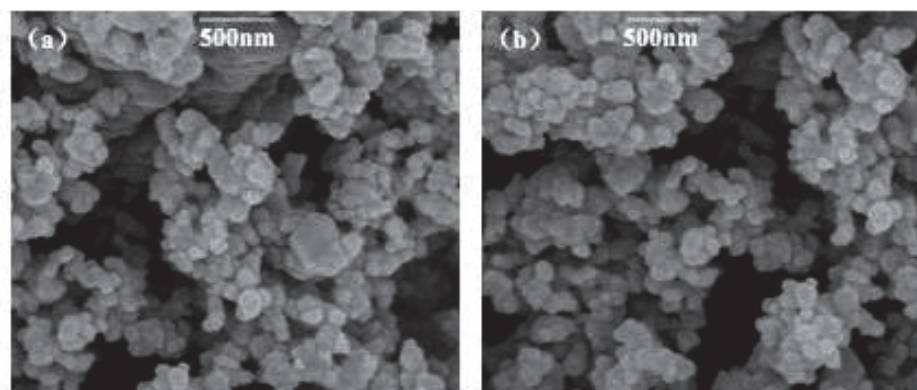


Fig. 3. SEM characterization over typically prepared Au(x)/Cu(8.0)CeO samples: a) Au(0.1)/Cu(8.0)CeO, b) Au(0.8)/Cu(8.0)CeO.

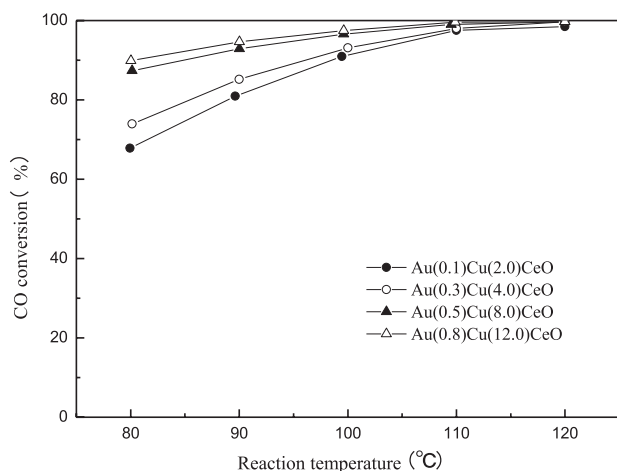


Fig. 4. The comparison on catalytic removal CO performed over Au(x)/Cu(8.0)CeO samples.

and partial oxidation of hydrocarbons, which met the quality requirement of proton exchange membrane fuel cell for the hydrogen source. Then, it could be safely concluded that the appropriate content of Au on Cu(8.0) CeO should be 0.52 (wt.%) considering its stability and cost of the catalyst. For the selective oxidation removal of CO with catalyst of Au(x)/Cu(8.0)CeO, further in-depth studies would be carried out such as XPS and in-situ FT-IR characterization in order to provide the basis for further scale-up experiment and industrial pilot testing.

Therefore, the intrinsic kinetics over Au(0.5)/Cu(8.0) CeO catalyst was further studied in a gradientless reactor as the sample had good performance on selective oxidation removal of CO in order to establish a feasible kinetic model, which could provide the basis for reactor design, simulation and catalyst engineering design as well as pilot industrial testing. Both of CO and H₂ could occur reaction with O₂ in the hydrogen rich atmosphere as follows.



It indicated that R₁ and R₂ are strong exothermic reactions, respectively, and then only the catalyst with good selectivity could promote the rate of R₁ reaction and inhibit the progress of R₂ reaction. Considering

Table 4. The table of orthogonal experimental factor levels.

Levels	Temperature (°C)	Molar ratio (O ₂ /CO)	Space velocity (h ⁻¹)
1	80	1.60	9800
2	90	1.25	8500
3	100	1.00	9000
4	110	0.80	9200

the dynamic model with the form of power function relative simple and also the influence of reaction component concentration and temperature on reaction rate was intuitive as well as the data processing and parameter estimation was relatively easy, the empirical model was chosen for the establishment of intrinsic kinetic mathematical model, and the power exponential rate equation was used to establish the kinetic equation. Based on the principle of not losing useful information and achieving the purpose of optimization with less experimental work, the table of orthogonal experimental factor levels was arranged (Table 4) to analyze the experimental data in order to obtain accurate dynamic equations. For reactions of R₁ and R₂, the power exponential kinetic equations was proposed as follows.

$$(-r_{\text{CO}}) = k_{01} e^{\frac{-E_1}{RT}} y_{\text{CO}}^{n_1} y_{\text{O}_2}^{n_2} \quad (1)$$

$$(-r_{\text{H}_2}) = k_{02} e^{\frac{-E_2}{RT}} y_{\text{H}_2}^{n_3} y_{\text{O}_2}^{n_4} \quad (2)$$

The following assumptions were made for the dynamic study on selective oxidation of CO over Au(0.5)/Cu(8.0)CeO catalyst. The experimental reactor was regarded as an ideal displacement reactor; the reactor was considered as an isothermal reactor, and the temperature in the reaction bed was equal; the pressure drop in the catalytic bed was very small, and the reaction was carried out under isobaric conditions; and the gas mixture in reaction system was as an ideal gas mixture. Based on the above basic assumptions, the key points of model selection and parameter estimation were as follows. The one-dimensional quasi homogeneous reactor model was used to describe the gas-solid catalytic reaction system. The model only involved the material balance equation without the equations of energy and momentum balance because the reaction process was isothermal and isobaric. The kinetic study was carried out under steady-state conditions, i.e. the compositions of the gas mixture only varied with the axial position of the reactor while the compositions at different radial positions were same and also independent of time.

According to the experimental data based on the designed orthogonal table and the basic assumptions of the kinetic model, the multivariate kinetic regression equations were obtained by MATLAB (MathWorks, USA) processing software as follows.

$$(-r_{\text{CO}}) = 0.084 e^{\frac{-103}{RT}} y_{\text{CO}}^{0.973} y_{\text{O}_2}^{-0.003} \quad (3)$$

$$(-r_{\text{H}_2}) = 0.059 e^{\frac{-1830}{RT}} y_{\text{H}_2}^{0.105} y_{\text{O}_2}^{-0.014} \quad (4)$$

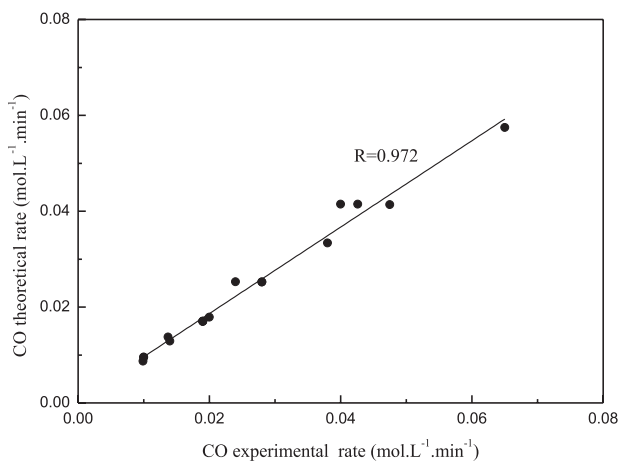


Fig. 5. The comparison of CO experimental and theoretical reaction rate over Au(0.5)/Cu(8.0)CeO catalyst.

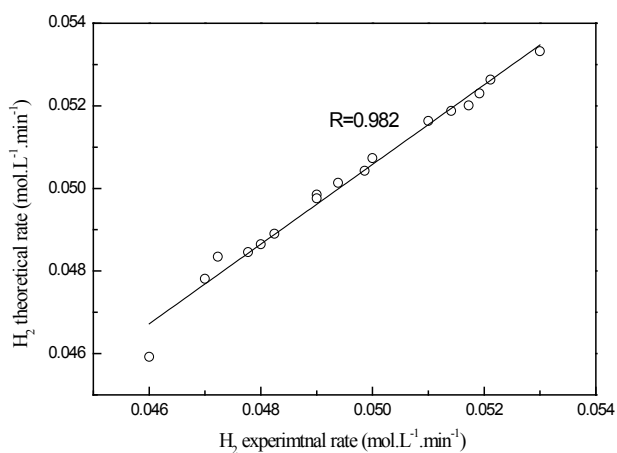


Fig. 6. The comparison of H₂ experimental and theoretical reaction rate over Au(0.5)/Cu(8.0)CeO catalyst.

The experimental reaction rates of CO and H₂ and the calculated values based on the kinetic models were shown in Figs 5 and 6, respectively. It showed that the experimental points were evenly distributed on both sides of the diagonal and also close to the diagonal indicating that the deviation between the calculated values of the model and the experimental values was very small, which meant that the correlation between them was good. Furthermore, it implied that the catalyst of Au(0.5)/Cu(8.0)CeO had relatively good selectivity for catalytic removal of CO in the H₂ rich atmosphere from the kinetic equations.

Conclusions

For the series of CuO-CeO₂ catalysts prepared by coprecipitation, BET characterization showed that the specific surface area and pore volume was the largest one when the content of Cu was 8.4(wt.%) on CuO-CeO₂

samples, while it decreased slightly when the content of Cu reached to 12.3 (wt.%) under the experimental prepared conditions. XRD characterization indicated that the crystal structure of CuO-CeO₂ catalysts was basically not varied at the range of 2.3~12.3 (wt.%) content of Cu except for the variation of XRD characteristic peak value. TPR showed that the catalysts of CuO-CeO₂ mainly appeared two characteristic peaks at the range of 60~400°C, i.e. low temperature α peak (160~180°C) and high temperature β peak (180~200°C). The ratio of $\alpha/(\alpha+\beta)$ was the largest when the content of Cu was 8.4 (wt.%) on CuO-CeO₂ samples, i.e. the catalyst of Cu(8.0)CeO, which was consistent with that its best activity under used experimental conditions. A series of catalysts of Au(x)/Cu(8.0)CeO were prepared by using Cu(8.0)CeO as precursor with impregnation method. SEM characterization showed that Au could evenly distributed on Cu(8.0)CeO with nano size under the prepared experimental conditions. The activity over the prepared series of Au(x)/Cu(8.0)CeO catalysts for selective oxidation removal of CO showed that the activity was increased with increasing Au loading, while its activity of Au(x)/Cu(8.0)CeO catalysts did not increase significantly when the Au loading was increased from 0.52(wt.%) to 0.78(wt.%). The concentration of CO at the outlet of reactor by using catalysts of Au(0.5)/Cu(8.0)CeO and Au(0.8)/Cu(8.0)CeO was less than 10ppm when the reaction temperature was close to 110°C, respectively. It could be safely concluded that the appropriate content of Au on Cu(8.0)CeO should be 0.52(wt.%) considering its stability and cost of the catalyst, i.e. Au(0.5)/Cu(8.0)CeO. The oxidation dynamics of CO and H₂ over Au(0.5)/Cu(8.0)CeO was measured in a gradientless reactor and the multiple kinetic regression equations of the oxidation reactions of CO and H₂ were obtained, respectively.

Acknowledgments

The authors gratefully appreciate the support in sample characterization by Tangshan Graphene Public Service Platform and Tangshan Key Laboratory of Chemical Environmental Protection and Film Materials, respectively.

References

1. DA SILVA VERAS T., MOZER T.S., DA SILVA CÉESAR A. Hydrogen: trends, production and characterization of the main process worldwide. *Int. J. Hydrogen Energy* **42** (4), 2018, **2017**.
2. ÖZGÜR T., YAKARYILMAZ A.C. A review: energy analysis of PEM and PEM fuel cell based CHP systems. *Int. J. Hydrogen Energy* **43**, 17993, **2018**.
3. DEVI A., SINGH A., BAJAR S., PANT D., DIN Z.U. Ethanol from lignocellulosic biomass: An in-depth analysis of pre-treatment methods, fermentation approaches

- and detoxification processes. *J. Environ. Chem. Eng.* **9** (5), 105798, **2021**.
4. PALANISAMY A., SOUNDARRAJAN N., RAMASAMY G. Analysis on production of bioethanol for hydrogen generation. *Environ. Sci. Pollut. Res.* **28**, 63690, **2021**.
 5. CHEN M.Q., LIANG D.F., WANG Y.S., WANG C.S., TANG Z.Y., LI C., HU J.X., CHENG W., YANG Z.L., ZHANG H., WANG J. Hydrogen production by ethanol steam reforming over M-Ni/sepiolite (M = La, Mg or Ca) catalysts. *Int. J. Hydrogen Energy* **46** (42), 21796, **2021**.
 6. SHARMA S., YASHWANTH P.K., ROY B. Deactivation study of the BICOVOX catalysts used in low temperature steam reforming of ethanol for H₂ production. *J. Phys. Chem. Solids* **156**, 110138, **2021**.
 7. DA SQ MENEZES J.P., MANFRO R.L., SOUZA M.M. V.M. Hydrogen production from glycerol steam reforming over nickel catalysts supported on alumina and niobia: deactivation process, effect of reaction conditions and kinetic modeling. *Int. J. Hydrogen Energy* **43** (32), 15064, **2018**.
 8. MORAES T.S., BORGES L.E.P., FARRAUTO R., NORONHA F.B. Steam reforming of ethanol on Rh/SiCeO₂ washed coated monolith catalyst: stable catalyst performance. *Int. J. Hydrogen Energy* **43** (1), 115, **2018**.
 9. MHADMHAN S., NATEWONG P., PRASONGTHUM N., SAMART C., REUBROYCHAROEN P. Investigation of Ni/SiO₂ fiber catalysts prepared by different methods on hydrogen production from ethanol steam reforming. *Catalysts* **8** (8), 319, **2018**.
 10. YAZICI M.S., DURSUN S., BORBÁTH I., TOMPOS A. Reformate gas composition and pressure effect on CO tolerant Pt/Ti_{0.8}Mo_{0.2}O₂-C electrocatalyst for PEM fuel cells. *Int. J. Hydrogen Energy* **46** (25), 13524, **2021**.
 11. BECKER H., BACQUART T., PERKINS M., MOORE N., IHONEN J., HINDS G., SMITH G. Operando characterisation of the impact of carbon monoxide on PEMFC performance using isotopic labelling and gas analysis. *J. Power Sources Advances* **6**, 100036, **2020**.
 12. GIANLUCA L., ALMERINDA DI B., LUCIANA L. Two-stage strategy for CO removal from H₂-rich streams over (nano-) CuO/CeO₂ structured catalyst at low temperature. *Appl. Sci.* **8** (5), 789, **2018**.
 13. SU H.Y., YU C.L., LIU J.X., ZHAO Y.H., MA X.F., LUO J., SUN C.H., LI W.X., SUN K.J. CO activation and methanation mechanism on hexagonal close-packed Co catalysts: effect of functionals, carbon deposition and surface structure. *Catal. Sci. Technol.* **10** (10), 3387, **2020**.
 14. EDWARD F.D., AMGAD E., KRISHNA R., ADARSH B. Life-cycle analysis of greenhouse gas emissions from hydrogen delivery: A cost-guided analysis. *Int. J. Hydrogen Energy* **46** (43), 22670, **2021**.
 15. YAN C., HAI H., GUO C., LI W., HUANG S., CHEN H. Hydrogen production by steam reforming of dimethyl ether and CO-PrOx in a metal foam micro-reactor. *Int. J. Hydrogen Energy* **39** (20), 10409, **2014**.
 16. ENGELHARDT P., MAXIMINI M., BECKMANN F., BRENNER M., MORITZ O. Coupled operation of a diesel steam reformer and an LT- and HT-PEFC. *Int. J. Hydrogen Energy* **39** (31), 18146, **2014**.
 17. LUKASHUK L., FÖTTINGER K., KOLAR E., RAMESHAN C., TSCHNER D., HÄVECKER M., KNOP-GERICKE A., YIGIT N., LI H., MCDERMOTTA E., STÖGER-POLLACH M., RUPPRECHTER G. Operando XAS and NAP-XPS studies of preferential CO oxidation on Co₃O₄ and CeO₂-Co₃O₄ catalysts. *J. Catal.* **344**, 1, **2016**.
 18. ABDELJAOUED A., RELVAS F., MENDES A., CHAHBANI M. Simulation and experimental results of a PSA process for production of hydrogen used in fuel cells. *J. Environ. Chem. Eng.* **6** (1), 338, **2018**.
 19. INABA M., ZHANG Z.G., MATSUOKA K., SONEDA Y. Effect of coexistence of siloxane on production of hydrogen and nanocarbon by methane decomposition using Fe catalyst. *Int. J. Hydrogen Energy* **46** (21), 11556, **2021**.
 20. MARQUARDT T., BODE A., KABELAC S. Hydrogen production by methane decomposition: Analysis of thermodynamic carbon properties and process evaluation. *Energ. Convers. Manage.* **221**, 113125, **2020**.
 21. CABALLERO M., DEL ANGEL G., RANGEL-VÁZQUEZ I., HUERTA L. Hydrogen production by methane decomposition on Pt/ γ -alumina doped with neodymium catalysts and its kinetic study. *Catal. Today* **349**, 106, **2020**.
 22. LAMY C. Electrocatalytic oxidation of low weight oxygenated organic compounds: A review on their use as a chemical source to produce either electricity in a Direct Oxidation Fuel Cell or clean hydrogen in an electrolysis cell. *J. Electroanal. Chem.* **875**, 114426, **2020**.
 23. SUH D.J., KWAK C., KIM J.H., KWON S.M., PARK T.J. Removal of carbon monoxide from hydrogen-rich fuels by selective low-temperature oxidation over base metal added platinum catalysts. *J. Power Sources* **142** (1-2), 70, **2005**.
 24. KIMURA M., MIYAO T., KOMORI S., CHEN A., HIGASHIYAMA K., YAMASHITA H., WATANABE M. Selective methanation of CO in hydrogen-rich gases involving large amounts of CO₂ over Ru-modified Ni-Al mixed oxide catalysts. *Appl. Catal. A: Gen.* **379** (1-2), 182, **2010**.
 25. SHEN L. M., ZHANG C., LIU Y. Meso-macroporous Al₂O₃ supported Ru catalysts for CO preferential oxidation in hydrogen-rich gases. *J. Nat. Gas Chem.* **21** (6), 653, **2012**.
 26. XI R.C., ZAO M.C., WEI M.L. Effect of La Addition on Ru/Al₂O₃ Catalyst for Selective CO Oxidation. *Adv. Mat. Res.* **347-353**, 3616, **2011**.
 27. ATEFEH T., NOUSHIN N., YADOLLAH M., ALI K.A. Cyclic molecular designed dispersion (CMDD) of Fe₂O₃ on CeO₂ promoted by Au for preferential CO oxidation in hydrogen. *Int. J. Hydrog. Energy* **45**, 33598, **2020**.
 28. YU H.B., GUO Z.T., WU C.Z., WANG S.J., LI B., YAN X.D., YAN B., YIN H.F. One-pot synthesis of Au-Fe₂O₃@SiO₂ core-shell nanoreactors for CO oxidation. *New J. Chem.* **44**, 5661, **2020**.
 29. BARBATO P.S., COLUSSI S., BENEDETTO A.D., LANDI G., TROVARELLI A. Origin of high activity and selectivity of CuO/CeO₂ catalysts prepared by solution combustion synthesis in CO-PROX reaction. *J. Phys. Chem. C* **120** (24), 13039, **2016**.
 30. WANG W.W., DU P.P., ZOU S.H., HE H.Y., WANG R.X., JIN Z., SHI S., HUANG Y.Y., SI S., SONG Q.S. Highly dispersed copper oxide clusters as active species in copper-ceria catalyst for preferential oxidation of carbon monoxide. *ACS Catal.* **5** (4), 2088, **2015**.
 31. ELIAS J.S., ARTRITH N., BUGNET M., GIORDANO L., BOTTON G.A., KOLPAK A.M., YANG S. H. Elucidating the nature of the active phase in copper/ceria catalysts for CO oxidation. *ACS Catal.* **6** (3), 1675, **2016**.
 32. DAVÓ-QUIÑONERO A., NAVLANI-GARCÍA M., LOZANO-CASTELLÓ D., BUENO-LÓPEZ A.,

- ANDERSON J.A. Role of hydroxyl groups in the preferential oxidation of CO over copper oxide-cerium oxide catalysts. *ACS Catal.* **6** (3), 1723, **2016**.
33. DU L.Y., WANG W.W., YAN H., WANG X., JIN Z., SONG Q.S., SI R., JIA C.J. Copper-ceria sheets catalysts: Effect of copper species on catalytic activity in CO oxidation reaction. *J. Rare Earth.* **35** (12), 1186, **2017**.
34. SHI L.M., GAO C.L., GUO F.H., WANG Y.J., ZHANG T.B. Catalytic performance of Zr-doped CuO-CeO₂ oxides for CO selective oxidation in H₂-rich stream. *J. Rare Earth.* **37** (7), 720, **2019**.
35. LANDI G., BENEDETTO A.D., COLUSSI S., BARBATO P.S., LISI L. Effect of carbon dioxide and water on the performances of an iron-promoted copper/ceria catalyst for CO preferential oxidation in H₂-rich streams. *Int. J. Hydrogen Energy* **41** (18), 7332, **2016**.
36. MALWADKAR S., BERA P., SATYANARAYANA C.V.V. Influence of cobalt on performance of Cu-CeO₂ catalysts for preferential oxidation of CO. *J. Rare Earth.* **38** (9), 941, **2020**.
37. CHEN F.Q., XIA Y., LAO J.Z., CHENG D.G., ZHAN X.L. Unraveling the change in multiple Cu species present in CuO/CeO₂ over the preferential CO oxidation reaction. *Ind. Eng. Chem. Res.* **60** (25), 9068, **2021**.
38. REN Y.Q. The preparation of M/CeO₂ (M = Au, Cu, Co) nanocatalysts and their catalytic performance for CO oxidation [D]. **2018**, Shandong University, Shandong, China.